

## Original Paper

# Fruit of *Phyllanthus emblica* L. suppresses macrophage foam-cell genesis and vascular lipid deposition using *in vivo* and *in vitro* models of early atherosclerosis development

Tao WU<sup>1</sup>, Xiaoyu LIU<sup>1</sup>, Zeyuan SUN<sup>1,2</sup>, Shu XING<sup>1\*</sup>, Liwen HAN<sup>3</sup>, Xiaobin LI<sup>4</sup>, Xuefang PAN<sup>1</sup>, Jianbin CHEN<sup>1</sup>, Mingyang ZHOU<sup>1</sup>, Tetiana DERKACH<sup>2</sup>, and John K. BIELICKI<sup>1\*</sup>

<sup>1</sup> School of Chemistry and Chemical Engineering, Qilu University of Technology (Shandong Academy of Sciences), 250353, Jinan, China

<sup>2</sup> Kyiv National University of Technologies and Design, 01011, Kyiv, Ukraine

<sup>3</sup> School of pharmacy and pharmaceutical sciences, Shandong first medical university & Shandong academy of medical sciences, 256200, Jinan, China

<sup>4</sup> Biology Institute, Qilu University of Technology (Shandong Academy of Sciences), 250103, Jinan, China

Received December 29, 2021 ; Accepted March 31, 2022

***Phyllanthus emblica* L. has been used for the prevention of cardiovascular disease, but its mechanisms remain unclear. In this study, fluorescence imaging in Zebrafish was used to screen phytomedicines for effects on atherosclerosis development *in vivo*. We found that an ethyl-acetate extract of *P. emblica* fruit (E-EA) proved highly effective for reducing vascular monocyte infiltration. The E-EA also reduced vascular cholesterol deposition in Zebrafish fed a high-fat diet. *In vitro*, E-EA suppressed the net deposition of cholesterol in macrophages in response to oxidized LDL. Suppression of macrophage foam-cell genesis resulted from substantial decrease in fluorescence-labelled-ox-LDL uptake as well as increased cholesterol efflux. Secretion of inflammatory cytokines from macrophages was also suppressed. QTOF-LC/MS revealed several unique compounds present in E-EA that have yet to be characterized for their anti-atherosclerosis effects. Our studies suggest that the fruit of *P. emblica* may suppress vascular lipid deposition by inhibiting macrophage recruitment and foam-cell genesis.**

Keywords: atherosclerosis, Ethnopharmacology, Cholesterol, Foam-cell, Macrophages

## Introduction

*Phyllanthus emblica* L. is a medicinal plant found in many tropical and subtropical areas throughout Asia and other parts of the world. The fresh fruit is often eaten directly or used to make various food products, such as juices and flavoured drinks that are increasing in popularity. The dried fruit, on the other hand, has long been used in Traditional Chinese Herbal Medicine (TCHM) known as Yuganzi. Traditional systems of Indian- (Ayurveda), Tibetan-, and Arab-medicine (Unani) have also frequently used *P. emblica* for the treatment of pharyngolaryngitis, gastroenteritis, skin sores, and wounds (Poltanov *et al.* 2009). Antioxidant properties of *P. emblica*

fruit have also been reported (Chen *et al.* 2019; Kim *et al.* 2005), and are thought to protect against liver disease and some forms of cancer (Zhao *et al.* 2015; Tung *et al.* 2018; Wang *et al.* 2017; Srinivasan *et al.* 2018; Chaphalkar *et al.* 2017; Usharani *et al.* 2013).

Recent clinical studies indicate the fruit of *Phyllanthus emblica* is able to reduce serum lipids and lessen the severity of oxidative stress in patients with metabolic syndrome (Upadya *et al.* 2019). Anti-diabetic action of *P. emblica* has also been described, further suggesting a cardiovascular benefit of the fruit (Usharani *et al.* 2019). Besides reducing lipid risk factors for cardiovascular disease, very little is

\*To whom correspondence should be addressed.

E-mail address: shuxing@qlu.edu.cn  
jkbielicki@hotmail.com

**Table 1.** Preparation of extracts from *Phyllanthus emblica* fruit.

Samples	Yield (% of original powder)	Total Phenolic Content (mg GE/g)	Total Flavonoid Content (mg RE/g)
Petroleum ether extract (E-PE)	0.7 ± 0.3	3.72 ± 0.25	3.71 ± 0.31
Chloroform extract (E-Ch)	1.1 ± 0.5	22.74 ± 2.52	7.07 ± 0.89
Ethyl acetate extract (E-EA)	3.6 ± 1.1	687.67 ± 55.23	135.47 ± 14.22
n-butanol extract (E-nBu)	4.6 ± 1.4	128.61 ± 10.87	23.00 ± 2.01
Aqueous extract (E-H <sub>2</sub> O)	4.1 ± 1.9	122.23 ± 11.89	22.66 ± 1.98

known about the effects of *P. emblica* fruit on atherosclerosis, i.e. a major form of cardiovascular disease. It has yet to be determined whether the fruit of *P. Emblica* is able to disrupt early stages of atherosclerosis development.

The development of atherosclerosis is complex, but it is characterized by the formation of macrophage foam-cells laden with cholesterol (Moore and Tabas 2011). Key events in foam-cell genesis involve the recruitment of monocyte-macrophages into the blood-vessel wall in response to inflammatory stimuli, followed by the deposition of cholesterol (Hansson 2005). The latter involves the unregulated uptake of modified lipoproteins by macrophages resulting in increased cholesterol content. This uptake is balanced by protective mechanisms that unload cholesterol from macrophages, a process known as cellular cholesterol efflux (Yvan-Charvet *et al.* 2010; Toh 2019).

Recently, the Zebrafish has emerged as a useful model for evaluating the effects of various agents on atherosclerosis development. This is due, in part, to the transparent nature of the larvae, which makes it feasible to visualize the vascular compartment in whole animals using real-time, fluorescence imaging techniques (Gut *et al.* 2017). Feeding Zebrafish a diet containing cholesterol produces hyperlipidaemia and lipoprotein oxidation (Fang *et al.* 2014). Consequently, cholesterol deposits in the vasculature mimicking the early stages of atherosclerosis seen in humans (Stoletov *et al.* 2009). The latter involves monocyte/macrophage migration into blood vessels (Wang *et al.* 2018).

In the present study, we employed *in vivo* Zebrafish models to investigate whether the fruit of *Phyllanthus emblica* impedes early steps in atherosclerosis development (Stoletov *et al.* 2009; d'Alencon *et al.* 2010). We found that polar extracts were highly effective at reducing monocyte migration into blood vessels. Substantial reduction in vascular cholesterol deposition was also noted with fruit extracts. Detailed studies in macrophages verified that the fruit of *Phyllanthus emblica* directly disrupted foam-cell genesis. The reduced lipid deposition in macrophages was related to an up-regulation of ABCG1 and cellular cholesterol efflux to HDL. QTOF-LC/MS identified potential candidates for exerting anti-atherosclerosis effects including a series of benzoate

metabolites.

## Materials and Methods

**Preparation of *Phyllanthus emblica* fruit extracts** Dried fruit of *Phyllanthus emblica* L., i.e. Yuganzi, was purchased from Tongrentang Pharmacy Ltd. (Beijing, China). The genus/species were confirmed by Dr. Liwen Han, an expert in Traditional Chinese Herbal Medicine and botanist. A sample (voucher# 2017-012-YGZ) of the Yuganzi used in this study has been kept in our laboratory in Qilu University of Technology for further analysis/verification as needed.

For experiments, the dried fruits were first powdered. The powder was sequentially extracted using a Soxhlet apparatus with petroleum ether, chloroform, ethyl acetate, n-butanol and finally deionized water. The powder -solvent ratio was 1:10 w/v. Each extract was concentrated under reduced pressure, vacuum dried (-20° C), then weighed to calculate yield (Table 1). The extracts were dissolved in dimethyl sulfoxide (DMSO; Sigma–Aldrich) for storage at a concentration of 10-100 mg/ml, and used at 1:1000 dilution ratio. DMSO (0.1 % final concentration) was used as a vehicle control.

**Zebrafish models** Zebrafish maintenance and procedures were conducted in accordance with the Guide for the Care and Use of Laboratory Animals published by the U.S. National Institutes of Health, and approved by the animal care and use committee of Qilu University of Technology (Shandong Academy of Sciences) (#SW20190601).

To evaluate lipid accumulation, *Tg(fli1:eGFP)* zebrafish larvae (green fluorescence expressed in endothelial cells) were used.(Stoletov *et al.* 2009) Five-day post-fertilized (5 dpf) zebrafish larvae were fed for 10 days a normal fish food or a high-cholesterol diet (HCD, normal food enriched with 3 % cholesterol). The food was supplemented with 10 µg/g of Cholesteryl BODIPY 542/563 C<sub>11</sub> (Thermo Fisher Scientific, USA).(Chen *et al.* 2015) E-EA was added directly into the fish-tank water (10 µg/ml final concentration) for 10 days of treatment. Similarly, parallel tanks of Zebrafish larvae were treated with 1 µM Ezetimibe as a positive control and 0.1 % DMSO as a vehicle control respectively. The red fluorescent intensity of caudal vasculature (starting after the cloacal) in zebrafish was quantified using a Nikon C1-si confocal-

microscope system.

To assess inflammation, *Tg (lyz:eGFP)* zebrafish larvae (green fluorescence expressed in monocyte/macrophages and granulocytes) were used. (d'Alencon *et al.* 2010) Three-day post-fertilized larvae were grouped and treated with 0.1 % DMSO, 10 µg/mL E-EA, or 20 µM ibuprofen (positive control) for 2 h, as described for the above cholesterol studies. The treated zebrafish were then stimulated with 20 µM CuSO<sub>4</sub> for 2h, in the continued presence of DMSO, E-EA or Ibuprofen, respectively. The migration of fluorescent inflammatory cells was imaged, and the number of inflammatory myeloid cells (green fluorescence) surrounding the lateral line neuromast cell area was counted.

#### *Determination of macrophage foam-cell formation*

Macrophage foam-like transition was evaluated by Oil-red O staining using a commercial kit (KeyGEN BioTech, China), according to the manufacturer's instructions. Briefly, RAW264.7 cells were treated with different extracts of emblica (10 µg/mL) or 0.1 % DMSO for 24 h. The treated cells were subsequently incubated with 50 µg/mL ox-LDL (Yiyuan Biotech., Guangdong, China) for another 24 h. Thereafter, cells were fixed and stained accordingly, and observed using Olympus DP 80 microscope (Olympus Corp., Japan). Relative differences between treatment groups was validated by extracting dye using 100 % isopropanol, and by measuring its absorbance at 518 nm using a SpectraMax M5 spectrophotometer. (Xie *et al.* 2018)

Macrophage free cholesterol (FC) and cholesterol ester (CE) mass were quantified to verify formation of foam-cells. To do this, we used enzymatic kits (SolarBio, Beijing, China) and following the protocol. (Carr *et al.* 1993) Briefly, RAW264.7 cells were treated with different extracts of emblica (10 µg/mL) or 0.1 % DMSO for 24 h, followed with 50µg/ml ox-LDL for another 48 h. The cells were then washed, homogenized, and the total cholesterol (TC) and free cholesterol (FC) quantified. A SpectraMax M5 spectrophotometer was employed to measure the absorbance of end-products. Results were reported as nmol cholesterol/mg cell protein. CE = TC - FC.

*Evaluation of ox-LDL uptake by macrophages* Uptake of ox-LDL by macrophages was evaluated using fluorescence Dil (1,1'-dioctadecyl-3,3,3',3'-tetramethylindocarbocyanine perchlorate) labelled ox-LDL, *i.e.* Dil-ox-LDL (Yiyuan Biotech., Guangdong, China). RAW264.7 cells were treated for 24h with E-EA or DMSO control, and then fed 50 µg/mL Dil-ox-LDL for 2 or 6 h in serum free RPMI 1640 medium. The cells were rinsed twice with ice-cold PBS, trypsinized, and mounted for flow-cytometry using FL-2 channel in FACS Caliber (Becton Dickinson, USA).

*Cholesterol efflux assay* Macrophage cholesterol efflux was determined using TopFluor-Cholesterol (Sigma-Aldrich,

USA) as a fluorescence probe. (Sankaranarayanan *et al.* 2011) RAW264.7 macrophages cultivated in 24-well plates (Costar) were labelled for 1 h with TopFluor-Cholesterol in RPMI 1640 medium containing 0.1 mM total cholesterol, where TopFluor-Cholesterol accounted for 37 % of the total cholesterol mass. After washing, labelled cells were incubated for 18 h with E-EA (5 µg/ml or 10 µg/ml), or 0.1 % DMSO in serum-free RPMI 1640 supplemented with 0.2 % BSA. 22-hydroxycholesterol and cis-retinoic acid (Sigma–Aldrich, each at 10 mM) treatment served as a positive control (PC). (Koldamova *et al.* 2003) The cells were washed and further incubated in serum-free RPMI 1640 containing 50 µg/mL HDL (Yiyuan Biotech., Guangdong, China) for 18h. The efflux media were removed, and centrifuged at 10,000 × g, 4 °C for 10 min. Cells were solubilized with 1 % cholic acid on a plate shaker for 4 h at room temperature. Fluorescence intensity of media and cells was monitored in SpectraMax M5 at λEx/Em=482/515 nm. Fractional efflux of cholesterol label was calculated as:

$$\% \text{ Efflux} = \text{FIM} / (\text{FIM} + \text{FIC}) * 100 \%$$

FIM: Fluorescence intensity of the media; FIC: Fluorescence intensity of the cells.

*Western blot analysis* The expression of ABC transporters and CD36 were examined by western blot analysis. RAW264.7 cells were treated with E-EA (5 µg/ml or 10 µg/ml) for 36 h. Addition of 22-hydroxycholesterol/cis-retinoic acid (each at 10 µM) was used as positive control (PC), while 0.1 % DMSO treatment served as a vehicle control. Anti-ABCA1 (AB18180, 1:500, Abcam), anti-ABCG1 (NB400-132, 1:500, Novus), anti-CD36 (18836-1-AP, 1:1000, ProteinTech.), and anti-α-Tubulin (11224-1-AP, 1:5000, ProteinTech.) were used as the primary antibodies. Horseradish peroxidase (HRP)-conjugated anti-rabbit (SA00001-2, 1:7500, ProteinTech.) was as secondary antibody. Proteins were visualized using Pierce ECL Plus Western Blotting Substrate (Thermo Fisher Scientific, USA) and a FlourChem HD2 imaging system (ProteinSimple Inc., USA).

*Determination of inflammatory cytokines secretion* RAW 264.7 cells were stimulated with 1µg/ml LPS for 24 h in the presence of E-EA or 0.1 % DMSO, with quercetin (QT, 10 µM) as a positive control. (Lee *et al.* 2018) After treatment, medium supernatants were collected and analysed by flow-cytometry using a BD Cytometric Bead Array (CBA) mouse inflammation kit.

*Cell viability assay and Determination of apoptosis* RAW264.7 or HUVECs were treated with 100 µg/ml ox-LDL for 24h with 5 or 10 µg/ml E-EA, or 0.1 % DMSO. Cell viability was assessed using 3-(4,5-dimethylthiazol-2-yl)-2,5-diphenyltetrazolium bromide (MTT) (Sigma–Aldrich). Cell apoptosis was quantified by flow-cytometry using a FITC-Annexin V/propidium iodide (PI) kit (KeyGEN BioTech,

China) following the manufacturer's instructions.

**Determination of total polyphenol and flavonoid content of extracts** The total polyphenol content of different extracts was examined with the Folin-Ciocalteu reagent, and the resulting blue complex was measured at 680 nm using a SpectraMax M5 spectrophotometer. (van Alstyne 1995) Gallic acid was used as a standard for the calibration curve, and the total polyphenol content was expressed as mg gallic acid equivalents (GE) per gram of dry weight of extract. The flavonoid content was examined by a commercial enzymatic kit (SolarBio, Beijing, China). The absorbance of the resulting complex was measured at 430 nm. Rutin was used as a standard for the calibration curve, and total flavonoid data were expressed in mg of rutin equivalents per gram of dry weight.

**QTOF-LC/MS characterization of the E-EA fraction** The characterization of E-EA was performed using QTOF-LC/MS (Agilent Technologies, USA). The separation of compounds was achieved on Waters Cortecs C18 2.1\*50mm 1.7 $\mu$ m column in gradient mode. Mobile phase A (water with 0.1 % formic acid) and mobile phase B (methanol) were set as follows: 70 % A – 30 % B (0-7 min), 60 % A – 40 % B (7-17 min), 20 % A – 80 % B (17-26 min), 10 % A – 90 % B (26-31min), with 4 min balance back to 90 % A- 10 % B. The injection volume was 20  $\mu$ L and flow rate was 0.3 ml/min. The mass spectra were acquired in ESI negative mode (100–1500 m/z). The parameters were as follows: drying gas (nitrogen) with flow rate of 15L/min; sheath gas temperature 350  $^{\circ}$ C, flow rate 12 L/min; voltage 3200V.

**Statistical analyses** Results were reported as means  $\pm$  SD. All experiments were repeated at least three times. One-way ANOVA followed by Turkey's multiple comparisons test were used to determine mean differences between groups, using GraphPad Prism software version 5 (GraphPad Software, CA). Statistical significance was defined as P-value < 0.05.

## Results

**Ethyl-acetate extract (E-EA) of *Phyllanthus emblica* L. reduced vascular –lipid and –inflammatory cell content** Zebrafish larvae *Tg (flil:eGFP)* fed a high-fat, cholesterol diet accumulate lipid in the vasculature, which can be visualized using a fluorescently labelled cholesterol probe. Treatment of fat-fed zebrafish with an ethyl-acetate extract (E-EA) from *Phyllanthus emblica* proved highly effective at reducing vascular lipid accumulation in blood vessels, as shown in Fig. 1A. E-EA significantly decreased fluorescent cholesterol accumulation in blood vessels to a level similar to that seen with Ezetimibe, a drug used in the treatment of hypercholesterolemia/cardiovascular disease.

To test if E-EA could modulate inflammatory responses *in vivo*, zebrafish larvae *Tg (lyz:eGFP)* were used that express

green fluorescence in monocytes/macrophages and granulocytes. As shown in Fig. 1B, E-EA treatment significantly inhibited the accumulation of inflammatory myeloid cells in the lateral line neuromast areas. Moreover, no increase in the death-rate of zebrafish larvae was observed among the treatment groups, indicating E-EA and the various test agents were well-tolerated (data not shown).

**Polar extracts from *Phyllanthus emblica* reduced foam-cell formation in macrophages** The *in vivo* zebrafish data suggested that extracts from *Phyllanthus emblica* may disrupt foam-cell genesis. This was tested using *in vitro* cell-culture models. Treatment of macrophages with ox-LDL resulted in the deposition of lipid and transition to a foam-like phenotype, as judged by Oil-red O staining seen in Fig. 2A. In contrast, polar extracts prepared with E-EA, E-nBu or E-H<sub>2</sub>O significantly decreased intracellular lipid levels caused by ox-LDL loading; in contrast, treatment with non-polar fractions (E-PE and E-Ch) did not. Results obtained with Oil-Red O staining were verified by measurement of cellular cholesterol mass. As shown in Fig. 2B, treatment of macrophages with the three polar extracts significantly reduced cellular cholesterol (FC) and cholesteryl ester (CE) content induced by ox-LDL. Among the extracts tested, the E-EA appeared to be most effective. The data indicate the polar extracts from *P. emblica*, particularly the E-EA extract, exerted direct effects on macrophages to reduce the foam-cell phenotype in response to ox-LDL.

**Oxidized LDL uptake and cholesterol efflux from macrophages** The net accumulation of cholesterol in macrophages is the result of a balance between ox-LDL uptake and cholesterol efflux. To discriminate between these possibilities, we performed ox-LDL uptake experiments, by treating macrophages with E-EA and measuring the uptake (2 and 6 hours) of fluorescence labelled ox-LDL, i.e. Dil-ox-LDL. As shown in Fig. 3A, E-EA slightly decreased cellular fluorescent intensity (-18.8 % at 2 h and -20.5 % at 6 h), indicative of a modest inhibition of ox-LDL uptake.

In contrast, E-EA treatment significantly increased HDL mediated cholesterol efflux in a dose-dependent manner; nearly a 2-fold increase in efflux was observed using 10  $\mu$ g/ml E-EA (Fig. 3B). This increase coincided with a 2-3 fold elevation in ABCA1 and ABCG1 protein expression with E-EA, i.e. cell-surface transporters for mediating cholesterol efflux. No change in the level of CD36, the main scavenger receptor mediating ox-LDL uptake, was noted (Fig. 3C). The latter is consistent with little change in ox-LDL uptake with fruit extracts. Together, these data suggest a prominent effect of E-EA on macrophages is related to increased cholesterol efflux mechanisms.

**E-EA reduced the secretion of pro-inflammatory cytokines from macrophages** To determine the effect of E-

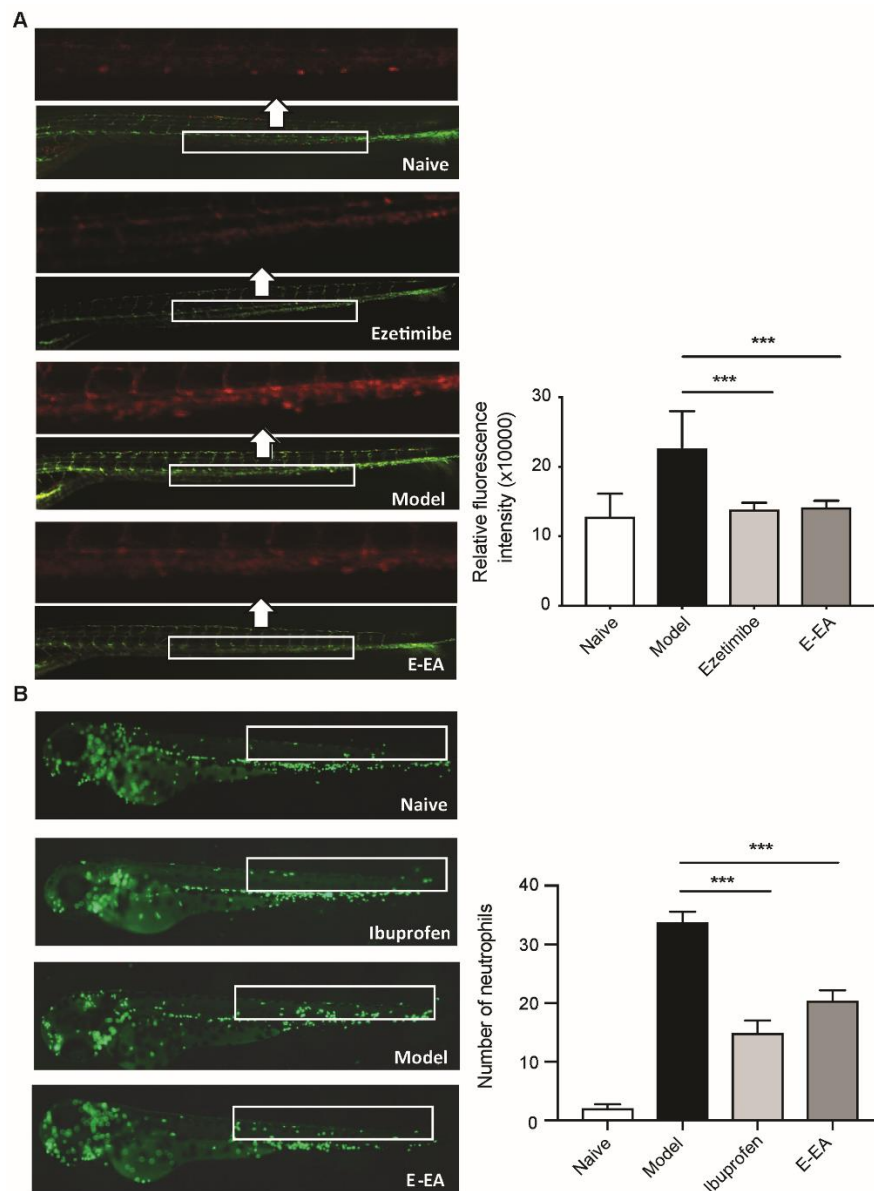


**Fig. 1.** E-EA reduced lipid- and inflammatory cells- accumulation in the vasculature of zebrafish.

In panel A, the vascular compartment of zebrafish was visualized by expression of green fluorescence protein in endothelial cells (*Tg flil:eGFP*) and BODIPY-cholesterol (542/563 red fluorescence) provided exogenously to assess lipid deposition. At 5 days post-fertilization, zebrafish were fed a standard food (naive group) or a high-cholesterol food + BODIPY-cholesterol (model group) for 10 days. Ezetimibe and E-EA were added to the tank water of high-cholesterol fed animals. Representative images (100x magnification) of the caudal plexus (highlighted boxes) are shown with green- and red-fluorescence merged. A higher magnification (300x) of the red fluorescence is shown above each image to facilitate group comparisons. The bar-graph shows quantitative data of the red fluorescence obtained from each group; values are means  $\pm$  SD, n=8 per group. \*\*\*  $p < 0.001$  compared to the model group. In Panel B, zebrafish expressing green fluorescence protein (*Tg lyz:eGFP*) in monocyte/macrophages and neutrophils were used to gauge an inflammatory response induced by copper. Zebrafish were treated with test agents together with  $\text{Cu}^{2+}$ , as described in the methods section. Images are at 100x magnification. The number of fluorescently-labelled immune cells migrating to the neuromast cell area (highlighted boxes) was counted to quantify the level of inflammation. Values are means  $\pm$ SD, n=8 per group. \*\*\*  $p < 0.001$  all compared to the model control group.

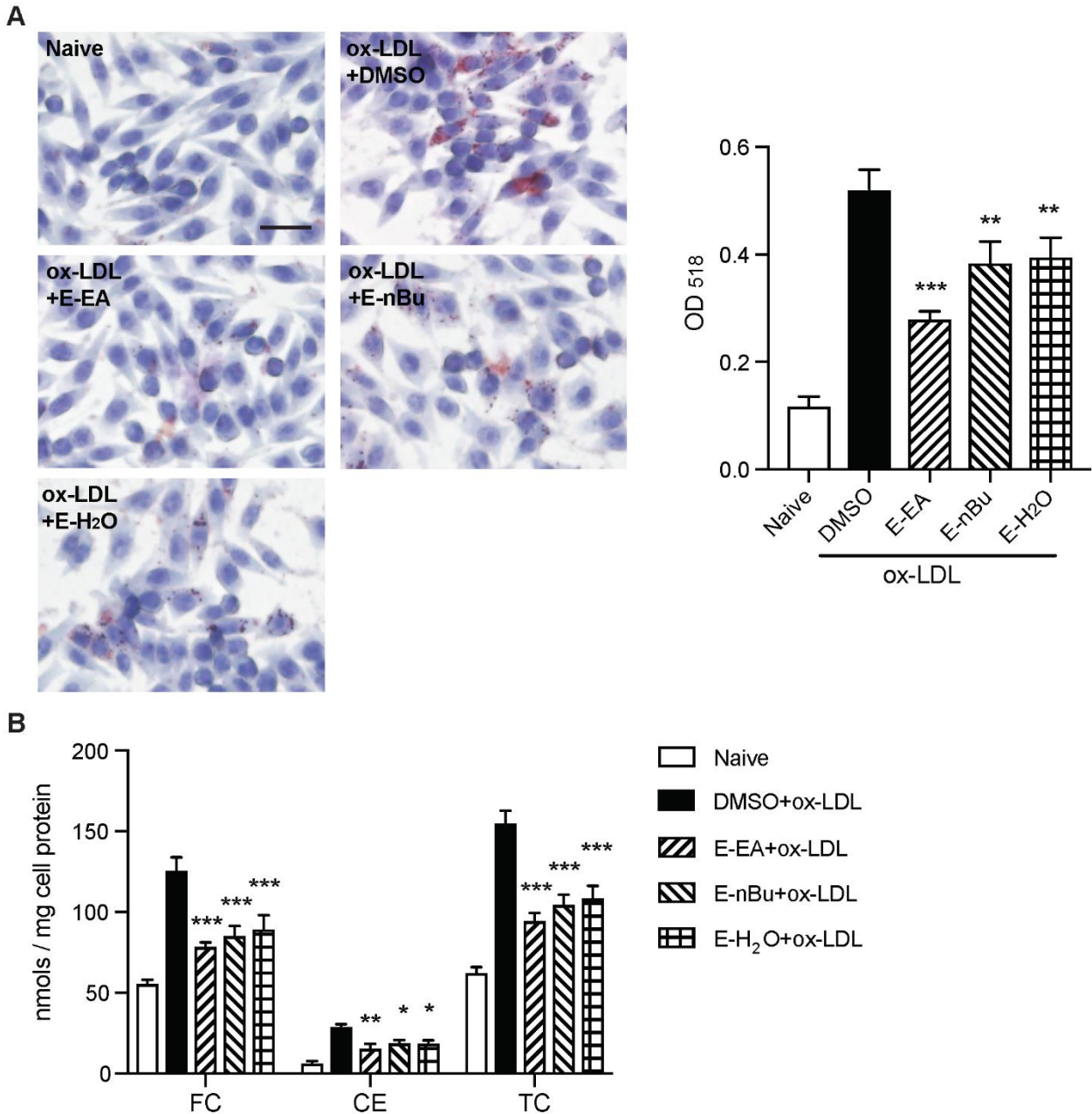


**Fig. 2.** Extracts of *Phyllanthus emblica* inhibited macrophage foam-like transition. RAW264.7 macrophages treated (24 h) with different extracts (10  $\mu\text{g}/\text{ml}$ ) from *Phyllanthus emblica* fruit or 0.1 % DMSO (vehicle control) were lipid-loaded by incubation (24 h) with ox-LDL (50  $\mu\text{g}/\text{ml}$ ). Panel A: in the images on the left, macrophages were stained with haematoxylin to visualize the nucleus (blue) and Oil-red O to visualize lipid droplets in the cytoplasm (arrows). Scale bar=50  $\mu\text{m}$ . In the bar-graph on the right, stained cells were dissolved in isopropanol, and the optical density (OD) at 518 nm was measured to determine Oil-red O intensity. Values are means  $\pm$ SD,  $n=3$  wells/group. \*\* $p < 0.01$  and \*\*\*  $p < 0.001$  compared to macrophages treated with DMSO + ox-LDL. Panel B: the mass of total cholesterol (TC) and free cholesterol (FC) in macrophages was quantified by enzymatic methods. Experiments were conducted as described in panel A, except oxidized LDL loading was for 48 h. Results were expressed as nmol of cholesterol per mg of cell protein; means  $\pm$ SD,  $n=3$  are shown. The amount of cholesterol esters (CE) was calculated by subtraction (TC-FC). \* $p < 0.05$ , \*\* $p < 0.01$ , and \*\*\*  $p < 0.001$  compared macrophages treated with DMSO + ox-LDL. E-EA: ethyl acetate extract; E-nBu: n-butanol extract; E-H<sub>2</sub>O: water extract.

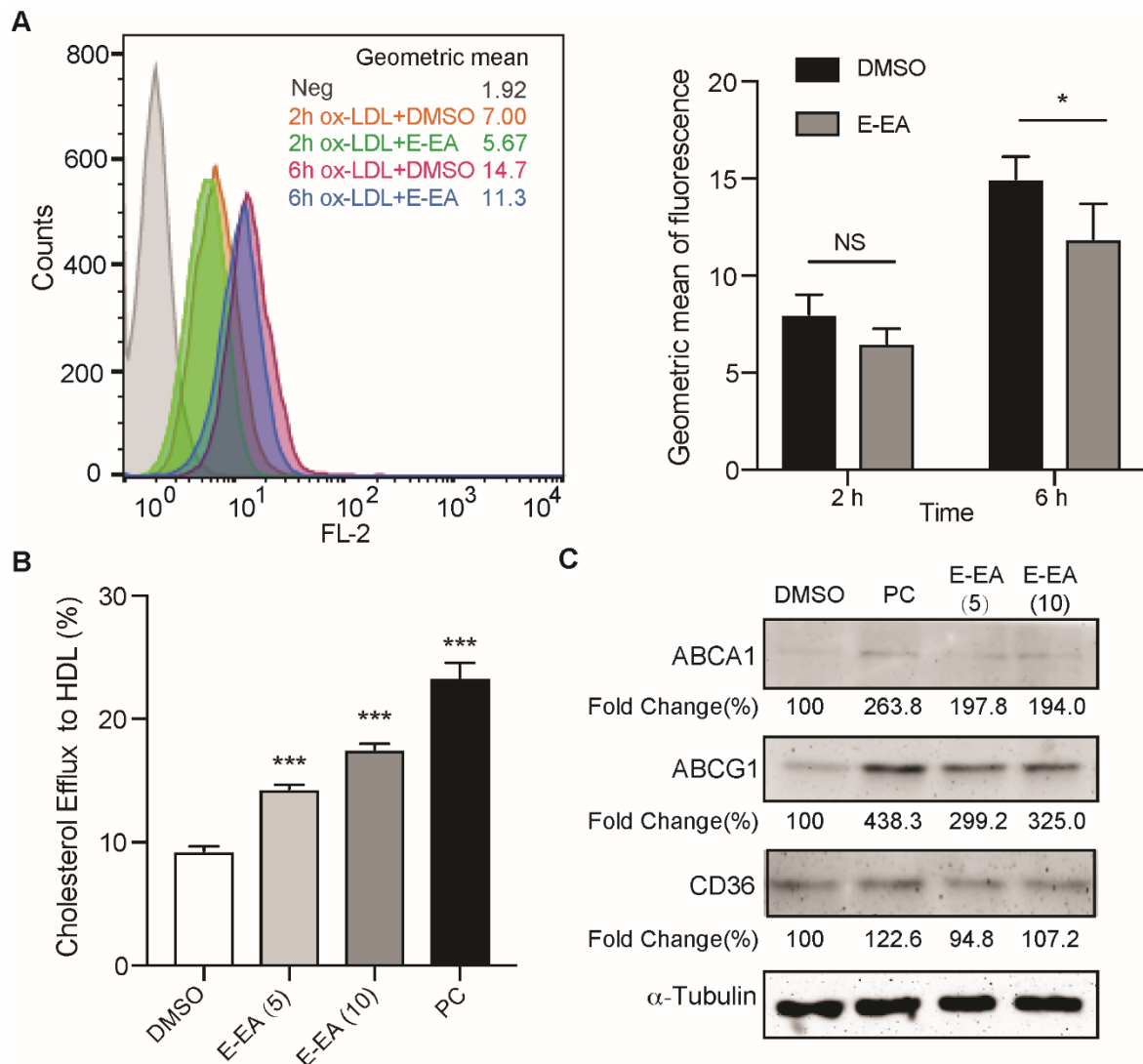


**Fig. 3.** Uptake of oxidized LDL and cholesterol efflux from macrophages.

RAW264.7 macrophages were treated (24 h) with E-EA (10  $\mu$ g/ml) or 0.1 % DMSO as a vehicle control. Panel A: Images on the left show the cellular uptake of DIL-ox-LDL (50  $\mu$ g/ml) following 2 or 6 h of incubation, respectively, as determined by flow-cytometry. Quantitative analysis of fluorescent geometric means is shown in the bar-graph on the right. Values are means  $\pm$  SD, n = 3. \* $p$ <0.05 compared to DMSO controls. NS = not significant. Panel B: Percent cholesterol efflux from cholesterol-labelled macrophages treated (18 h) with E-EA (5 or 10  $\mu$ g/ml). HDL was used as an acceptors in the medium (50  $\mu$ g/ml) and cholesterol efflux measured at 18 h, as described in the methods section. Values are means  $\pm$ SD, n = 3. \*\*\* $p$ <0.001 compared to 0.1 % DMSO control. Panel C: Western-blot analysis showing relative levels of ABCA1, ABCG1 and CD35 protein mass in RAW264.7 macrophages treated with the indicated agents for 36 hours. A representative image is shown.  $\alpha$ -tubulin was measured to verify total-protein loads were identical in all lanes. Fold change in protein levels were determined by densitometry, normalizing to the DMSO control group (i.e. set at 100 %).

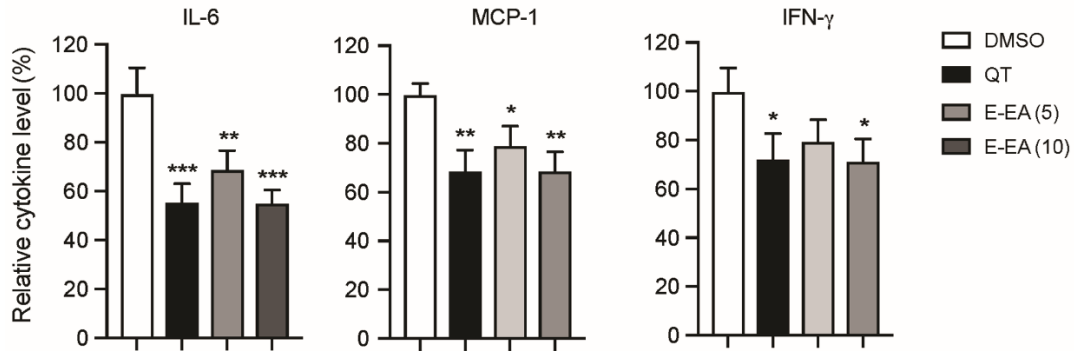


**Fig. 4.** E-EA suppressed inflammatory cytokine secretion from macrophages.

RAW-264.7 macrophages were treated (24 h) with LPS (1  $\mu\text{g}/\text{ml}$ ) in the absence or presence of E-EA (5  $\mu\text{g}/\text{ml}$  or 10  $\mu\text{g}/\text{ml}$ ). Quercetin (QT, 10  $\mu\text{M}$ ) served as the positive control. The cytokine concentration in the medium was determined using a BD Cytometric Bead Array via flow-cytometry ( $n = 3$ ). Cytokine secretion level of the DMSO group was set at 100%. \* $p < 0.05$ , \*\* $p < 0.01$ , and \*\*\* $p < 0.001$  vs. DMSO treated macrophages + LPS.

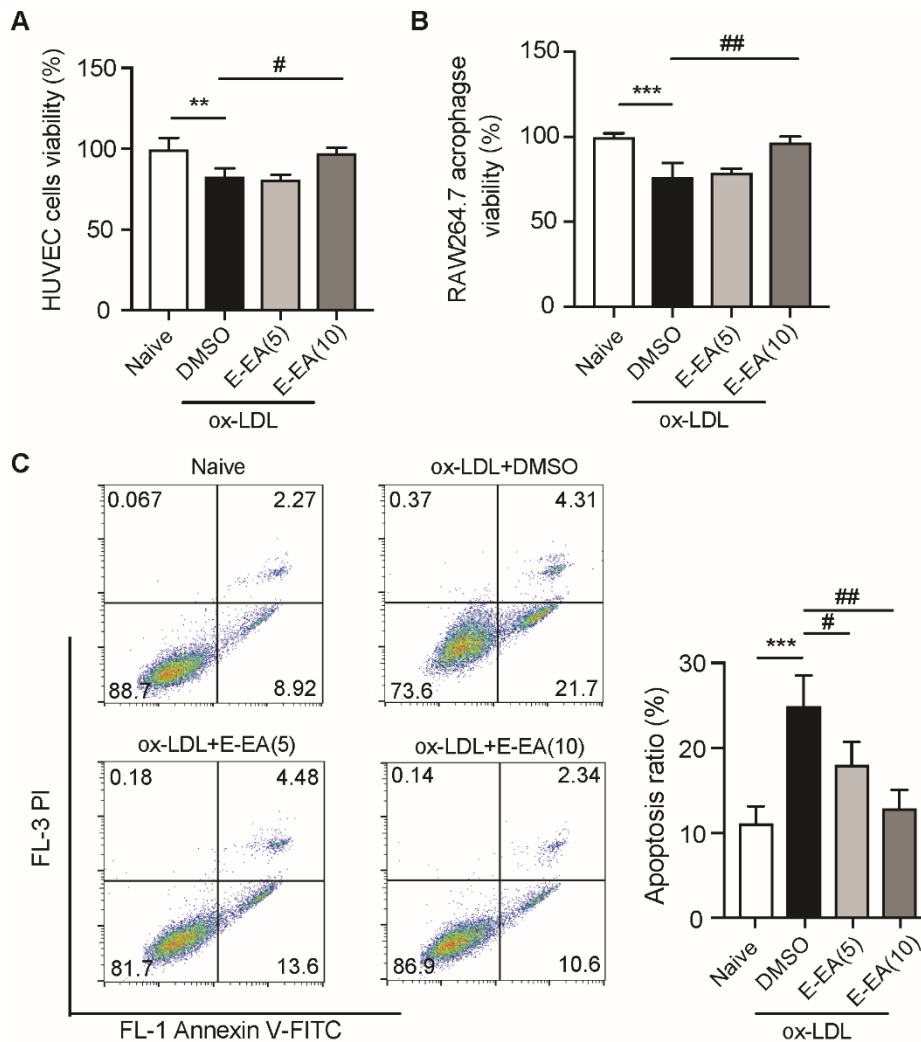


**Fig. 5.** E-EA protected cells from ox-LDL induced cytotoxicity.

Human umbilical vein endothelia cells, i.e. HUVECs (Panel A), and RAW264.7 macrophages (Panel B) were treated (24 h) with ox-LDL (100  $\mu\text{g}/\text{ml}$ ) in the absence and presence of E-EA (5  $\mu\text{g}/\text{ml}$  or 10  $\mu\text{g}/\text{ml}$ ). Cell viability was examined by MTT assay ( $n = 3$ ). Panel C: Effect of E-EA on apoptosis induced by ox-LDL in RAW264.7 macrophages. Cells were treated as in panel 5B. Annexin V-FITC & PI kits were used to analyse apoptosis via flow-cytometry. Representative image of flow-cytometry diagram (left panel) and quantitative analysis of apoptotic ratio from 3 independent experiments (right panel) are shown. The lower right quadrant represents cells in early-to-late apoptosis, whereas the upper right quadrant corresponds to cells in late apoptosis or secondary necrosis. \*\* $p < 0.01$  and \*\*\* $p < 0.001$  compared between the vehicle alone group (i.e. 0.1% DMSO = naïve group) and the DMSO + ox-LDL group; and # $p < 0.05$ , and ## $p < 0.01$  for DMSO + ox-LDL group versus E-EA treatment groups.

**Table 2.** Top ten abundant compounds characterized by QTOF-LC/MS in E-EA.

Abundance sequence	Name	Formula	Retention time	M. wt (g/mol)	Difference (ppm)
1	5-Hydroxyisophthalic acid	C <sub>8</sub> H <sub>6</sub> O <sub>5</sub>	1.56	182.0215	2.3
2	Amlaic acid	C <sub>27</sub> H <sub>24</sub> O <sub>19</sub>	3.073	652.0912	1.14
3	3,5-Dihydroxybenzoic acid	C <sub>7</sub> H <sub>6</sub> O <sub>4</sub>	1.476	154.0266	-0.78
4	10-Gingerdione	C <sub>21</sub> H <sub>32</sub> O <sub>4</sub>	22.654	348.2301	0.66
5	6-Methylgingediacetate	C <sub>22</sub> H <sub>34</sub> O <sub>6</sub>	22.654	394.2355	0.58
6	Ethyl gallate	C <sub>9</sub> H <sub>10</sub> O <sub>5</sub>	3.409	198.0528	3.66
7	(-)-1,10-Epoxy-guaia-11-ene	C <sub>15</sub> H <sub>24</sub> O	21.898	220.1827	0.66
8	7 $\alpha$ -Hydroxycholesterol	C <sub>28</sub> H <sub>48</sub> O <sub>2</sub>	28.453	416.3654	0.48
9	Irisoquin F	C <sub>29</sub> H <sub>50</sub> O <sub>4</sub>	28.453	462.3709	0.44
10	2'-Hydroxycinnamaldehyde	C <sub>9</sub> H <sub>8</sub> O <sub>2</sub>	7.107	148.0524	3.1

EA on inflammatory responses of macrophages, RAW264.7 cells were stimulated by LPS in the presence or absence of E-EA. Quercetin (QT, 10  $\mu$ M), which has been reported with anti-inflammatory function, was used as the positive control. The cytokine concentration in culture medium was determined using a BD Cytometric Bead Array. As seen in Fig. 4, E-EA treatment significantly decreased the secretion of IL-6, MCP-1 and IFN- $\gamma$ . No significant effect of E-EA was observed on the secretion of IL-12, p70, IL-10 or TNF (data not shown). These data suggest that E-EA could alleviate the pro-inflammatory responses of macrophages.

*E-EA protected macrophages and endothelial cells from ox-LDL induced cytotoxicity* Incubation of macrophages or endothelial cells for 24 h with oxidized LDL (100  $\mu$ g/ml) produced a small but significant decrease (25%) in cell viability compared to control cells treated with vehicle alone (Fig. 5A and 5B). The cytotoxicity of ox-LDL was associated with induction of apoptosis, as shown in Fig. 5C. In contrast, the presence of the higher dose of E-EA (10  $\mu$ g/ml) afforded protection against cytotoxic and apoptotic responses of ox-LDL (Fig. 5C). Moreover, treatment of cells with the different extracts alone did not alter cell viability (data not shown), indicating the extracts prepared from the *P. emblica* fruit were not in-and-of-themselves harmful to the cells.

*Characterization of E-EA* Chemical analyses were performed to identify components of the biologically active E-EA extract. Most of the compounds identified were relatively polar, consistent with the nature of the extraction solvent and the total polyphenol/flavonoid contents (Table 1). The top 10 most abundant compounds identified by QTOF-LC/MS are shown in Table 2. Many of the compounds were benzoate metabolites. Among the most noted were ethyl gallate, 5-hydroxyisophthalic acid, and 3-5 dihydroxybenzoic acid. The sterol 7 $\alpha$ -hydroxycholesterol, a well-known modulator of lipid

homeostasis, was also identified. Representative chromatographs of the individual mass spectra can be found with supplementary data.

## Discussion

In the present study, we employed *in vivo* screening methods to determine whether the fruit of *Phyllanthus emblica* influences early events in atherosclerosis development. Cell-culture studies were subsequently performed to support the *in vivo* findings and further explore the potential mechanisms.

We found that treating zebrafish larvae with *Phyllanthus emblica* extracts (E-EA) reduced the infiltration of inflammatory cells, including monocyte/macrophages, into the vasculature in response to copper-mediated oxidation. Reduced inflammatory cell migration was associated with a parallel reduction in cholesterol deposition *in vivo*, which suggested that the formation of macrophage foam-cells may be suppressed by the fruit extracts in light of the hyperlipidaemic, high-fat diet challenge.

Suppression of inflammatory cell migration and reduced lipid deposition are consistent with the notion that the fruit of *P. emblica* altered the behaviour of monocyte/macrophages *in vivo*. Such effects could be related to direct action of the fruit on macrophages or indirect effects. To discriminate between these two possibilities, we directly exposed macrophages growing in culture to extracts of *P. emblica* and analysed the extent of lipid deposition in response to oxidized LDL. Substantial reductions in foam-cell formation were noted with macrophages treated with extracts, particularly the E-EA.

The ability of fruit extracts to reduce lipid-deposition in macrophages was largely independent of lipid uptake, as the levels of cell-surface CD36 were unaffected by the biologically active E-EA extract. (Terra *et al.* 2009) Moreover, lipid uptake measured directly using Dil-ox-LDL (oxidized

LDL labelled with the fluorescent dye DiI) was only modestly reduced (18 - 22%) with E-EA compared to controls. This small, fractional reduction in uptake could not account for the relatively large decrease (~2-fold) in overall lipid deposition observed with the E-EA extract. The latter suggests other mechanisms were likely involved to reduce net lipid accumulation in macrophages.

Stimulation of cellular cholesterol efflux is thought to represent a viable pathway for reducing macrophage lipid stores and protecting against foam-cell formation.(Gao *et al.* 2016; Zhao *et al.* 2016) Therefore, we evaluated whether treatment of macrophages with fruit extracts increased cellular cholesterol efflux. We found that substantial (2 to 3 fold) increases in cholesterol efflux were observed to high density lipoproteins (HDL). This increase was accompanied by a parallel increase in the mass of ABCG1 protein, a major membrane transporter involved in facilitating cholesterol efflux to HDL.(Yvan-Charvet *et al.* 2010) We also measured increased expression of ABCA1 in macrophages with E-EA treatment. However, the overall level of ABCA1 expression was relatively low and cholesterol efflux to lipid-free apolipoprotein A-I (the major ligand for ABCA1) was only modestly increased. As a result, there appears to be differences in the response of the cholesterol efflux pathways that were up-regulated by E-EA, whereby an increase in the HDL mediated pathway involving ABCG1 seemed most responsive to the fruit extracts.

Direct exposure of macrophages to extracts of *P. emblica* fruit also reduced inflammatory cytokine secretion. Most noted was a significant reduction in the secretion of IL-6 and MCP-1 in response to LPS stimulation. MCP-1 is thought to be involved in the initial stages of atherosclerosis, because it functions as a chemotactic protein to recruit monocyte/macrophages into the vascular wall.(Lin *et al.* 2014) Thus, it would appear that the fruit of *P. emblica* may exert several effects on early atherosclerosis development, involving suppression of inflammatory cell migration/monocyte recruitment and stimulation of cholesterol efflux mechanisms from macrophages.

QTOF-LC/MS analysis of the biologically active E-EA extract revealed several compounds in high abundance (Table 2). Interestingly, one of these compounds was the benzoate plant metabolite ethyl gallate, which we have previously found to reduce atherosclerosis development in apolipoprotein E deficient mice.(Liu *et al.* 2021) This evidence indicates that ethyl gallate may represent one of the active components of the *P. emblica* fruit responsible for its anti-atherosclerosis effects. In addition, the compounds 10-gingerdione and 2-hydroxycinnamaldehyde we tentatively identified could also be involved in the anti-atherosclerosis effects of E-EA. These compounds are thought to possess anti-oxidative and anti-

inflammatory properties.(van Breemen *et al.* 2011; Lee *et al.* 2005; Yoon *et al.* 2019) The latter involves suppression of inflammatory cytokine secretion from macrophages.(Lee *et al.* 2005) Yet, the biological effects of other compounds we found in E-EA, such as 5-hydroxyisophthalic acid, 6-Methylgingediacetate, and Irisoquin F, are currently not known. It is left to be determined whether these compounds that were present share similar or more potent effects to disrupt atherosclerosis development.

In conclusion, the present study suggests that the fruit of *Phyllanthus emblica* exerts beneficial effects to reduce early atherosclerosis development. Major effects of the fruit appeared to be related to decreased persistence of inflammatory responses and reduced vascular lipid deposition. The underlying mechanisms were related to inhibited foam-cell genesis and reduced inflammatory cytokine secretion from macrophages. Further studies of the active components of *P. emblica* fruit are warranted to identify candidate compounds for use as potential treatments for cardiovascular diseases such as atherosclerosis.

**Acknowledgements** This research was supported by grants from Natural Science Foundation of Shandong Province, China (funding number: ZR2017BH053); Joint Research Fund for Young Doctors of Qilu University of Technology (Shandong Academy of Sciences) (funding number: 2017BSH2017, and 2017BSH2016), and International Cooperation Fund of Qilu University of Technology (Shandong Academy of Sciences) (funding number QLUTGJHZ2018002).

**Conflict of interest** There are no conflicts of interest to declare.

**Ethical statement** Zebrafish maintenance and procedures were conducted in accordance with the Guide for the Care and Use of Laboratory Animals published by the U.S. National Institutes of Health, and approved by the animal care and use committee of Qilu University of Technology (Shandong Academy of Sciences) (#SW20190601).

## References

- Carr, T.P., Andresen, C.J., and Rudel, L.L. (1993). Enzymatic determination of triglyceride, free cholesterol, and total cholesterol in tissue lipid extracts. *Clin Biochem*, **26**, 39–42.
- Chaphalkar, R., Apte, K.G., Talekar, Y., Ojha, S.K., and Nandave, M. (2017). Antioxidants of *Phyllanthus emblica* L. Bark Extract Provide Hepatoprotection against Ethanol-Induced Hepatic Damage: A Comparison with Silymarin. *Oxid Med Cell Longev*, **2017**, 3876040, 1–10.
- Chen, K., Wang, C.Q., Fan, Y.Q., Xie, Y.S., Yin, Z.F., Xu,

- Z.J., Zhang, H.L., Cao, J.T., Han, Z.H., Wang, Y., and Song, D.Q. (2015). Optimizing methods for the study of intravascular lipid metabolism in zebrafish. *Mol Med Rep*, **11**, 1871–1876.
- Chen, L., Wu, X., Shen, T., Wang, X., Wang, S., Wang, J., and Ren, D. (2019). Protective effects of ethyl gallate on H<sub>2</sub>O<sub>2</sub>-induced mitochondrial dysfunction in PC12 cells. *Metab Brain Dis*, **34**, 545–555.
- d'Alencon, C.A., Pena, O.A., Wittmann, C., Gallardo, V.E., Jones, R.A., Loosli, F., Liebel, U., Grabher, C., and Allende, M.L. (2010). A high-throughput chemically induced inflammation assay in zebrafish. *BMC Biol*, **8**, 151–167.
- Fang, L., Liu, C., and Miller, Y.I. (2014). Zebrafish models of dyslipidemia: relevance to atherosclerosis and angiogenesis. *Transl Res*, **163**, 99–108.
- Gao, H., Li, L., Li, L., Gong, B., Dong, P., Fordjour, P.A., Zhu, Y., and Fan, G. (2016). Danshensu Promotes Cholesterol Efflux in RAW264.7 Macrophages. *Lipids*, **51**, 1083–1092.
- Gut, P., Reischauer, S., Stainier, D.Y.R., and Arnaout, R. (2017). Little Fish, Big Data: Zebrafish as a Model for Cardiovascular and Metabolic Disease. *Physiol Rev*, **97**, 889–938.
- Hansson, G.K. (2005). Inflammation, atherosclerosis, and coronary artery disease. *N Engl J Med*, **352**, 1685–95.
- Kim, H.J., Yokozawa, T., Kim, H.Y., Tohda, C., Rao, T.P., and Juneja, L.R. (2005). Influence of amla (*Embllica officinalis* Gaertn.) on hypercholesterolemia and lipid peroxidation in cholesterol-fed rats. *J Nutr Sci Vitaminol (Tokyo)*, **51**, 413–418.
- Koldamova, R.P., Lefterov, I.M., Ikonovic, M.D., Skoko, J., Lefterov, P.I., Isanski, B.A., DeKosky, S.T., and Lazo, J.S. (2003). 22R-hydroxycholesterol and 9-cis-retinoic acid induce ATP-binding cassette transporter A1 expression and cholesterol efflux in brain cells and decrease amyloid beta secretion. *J Biol Chem*, **278**, 13244–13256.
- Lee, H.N., Shin, S.A., Choo, G.S., Kim, H.J., Park, Y.S., Kim, B.S., Kim, S.K., Cho, S.D., Nam, J.S., Choi, C.S., Che, J.H., Park, B.K., and Jung, J.Y. (2018). Antiinflammatory effect of quercetin and galangin in LPSstimulated RAW264.7 macrophages and DNCB-induced atopic dermatitis animal models. *Int J Mol Med*, **41**, 888–898.
- Lee, S.H., Lee, S.Y., Son, D.J., Lee, H., Yoo, H.S., Song, S., Oh, K.W., Han, D.C., Kwon, B.M., and Hong, J.T. (2005). Inhibitory effect of 2'-hydroxycinnamaldehyde on nitric oxide production through inhibition of NF-kappa B activation in RAW 264.7 cells. *Biochem Pharmacol*, **69**, 791–799.
- Lin, J., Kakkar, V., and Lu, X. (2014). Impact of MCP-1 in atherosclerosis. *Curr Pharm Des*, **20**, 4580–4588.
- Liu, W., Liu, J., Xing, S., Pan, X., Wei, S., Zhou, M., Li, Z., Wang, L., and Bielicki, J.K. (2021). The benzoate plant metabolite ethyl gallate prevents cellular- and vascular-lipid accumulation in experimental models of atherosclerosis. *Biochem Biophys Res Commun*, **556**, 65–71.
- Moore, K.J., and Tabas, I. (2011). Macrophages in the pathogenesis of atherosclerosis. *Cell*, **145**, 341–355.
- Poltanov, E.A., Shikov, A.N., Dorman, H.J., Pozharitskaya, O.N., Makarov, V.G., Tikhonov, V.P., and Hiltunen, R. (2009). Chemical and antioxidant evaluation of Indian gooseberry (*Embllica officinalis* Gaertn., syn. *Phyllanthus emblica* L.) supplements. *Phytother Res*, **23**, 1309–1315.
- Sankaranarayanan, S., Kellner-Weibel, G., de la Llera-Moya, M., Phillips, M.C., Asztalos, B.F., Bittman, R., and Rothblat, G.H. (2011). A sensitive assay for ABCA1-mediated cholesterol efflux using BODIPY-cholesterol. *J Lipid Res*, **52**, 2332–2340.
- Srinivasan, P., Vijayakumar, S., Kothandaraman, S., and Palani, M. (2018). Anti-diabetic activity of quercetin extracted from *Phyllanthus emblica* L. fruit: In silico and in vivo approaches. *J Pharm Anal*, **8**, 109–118.
- Stoletov, K., Fang, L., Choi, S.H., Hartvigsen, K., Hansen, L.F., Hall, C., Pattison, J., Juliano, J., Miller, E.R., Almazan, F., Crosier, P., Witztum, J.L., Klemke, R.L., and Miller, Y.I. (2009). Vascular lipid accumulation, lipoprotein oxidation, and macrophage lipid uptake in hypercholesterolemic zebrafish. *Circ Res*, **104**, 952–960.
- Terra, X., Fernandez-Larrea, J., Pujadas, G., Ardevol, A., Blade, C., Salvado, J., Arola, L., and Blay, M. (2009). Inhibitory effects of grape seed procyanidins on foam cell formation in vitro. *J Agric Food Chem*, **57**, 2588–2594.
- Toh, R. (2019). Assessment of HDL Cholesterol Removal Capacity: Toward Clinical Application. *J Atheroscler Thromb*, **26**, 111–120.
- Tung, Y.T., Huang, C.Z., Lin, J.H., and Yen, G.C. (2018). Effect of *Phyllanthus emblica* L. fruit on methionine and choline-deficiency diet-induced nonalcoholic steatohepatitis. *J Food Drug Anal*, **26**, 1245–1252.
- Upadya, H., Prabhu, S., Prasad, A., Subramanian, D., Gupta, S., and Goel, A. (2019). A randomized, double blind, placebo controlled, multicenter clinical trial to assess the efficacy and safety of *Embllica officinalis* extract in patients with dyslipidemia. *BMC Complement Altern Med*, **19**, 27–40.
- Usharani, P., Fatima, N., and Muralidhar, N. (2013). Effects of *Phyllanthus emblica* extract on endothelial dysfunction and biomarkers of oxidative stress in patients with type 2 diabetes mellitus: a randomized, double-blind, controlled study. *Diabetes Metab Syndr Obes*, **6**, 275–284.
- Usharani, P., Merugu, P.L., and Nutalapati, C. (2019). Evaluation of the effects of a standardized aqueous extract of *Phyllanthus emblica* fruits on endothelial dysfunction, oxidative stress, systemic inflammation and lipid profile in

- subjects with metabolic syndrome: a randomised, double blind, placebo controlled clinical study. *BMC Complement Altern Med*, **19**, 97–105.
- van Alstyne, K.L. (1995). Comparison of three methods for quantifying brown algal polyphenolic compounds. *J Chem Ecol*, **21**, 45–58.
- van Breemen, R.B., Tao, Y., and Li, W. (2011). Cyclooxygenase-2 inhibitors in ginger (*Zingiber officinale*). *Fitoterapia*, **82**, 38–43.
- Wang, C., Niimi, M., Watanabe, T., Wang, Y., Liang, J., and Fan, J. (2018). Treatment of atherosclerosis by traditional Chinese medicine: Questions and quandaries. *Atherosclerosis*, **277**, 136–144.
- Wang, C.C., Yuan, J.R., Wang, C.F., Yang, N., Chen, J., Liu, D., Song, J., Feng, L., Tan, X.B., and Jia, X.B. (2017). Anti-inflammatory Effects of *Phyllanthus emblica* L on Benzopyrene-Induced Precancerous Lung Lesion by Regulating the IL-1beta/miR-101/Lin28B Signaling Pathway. *Integr Cancer Ther*, **16**, 505–515.
- Xie, Z., Wang, X., Liu, X., Du, H., Sun, C., Shao, X., Tian, J., Gu, X., Wang, H., Tian, J., and Yu, B. (2018). Adipose-Derived Exosomes Exert Proatherogenic Effects by Regulating Macrophage Foam Cell Formation and Polarization. *J Am Heart Assoc*, **7**, e007442
- Yoon, Y.J., Kim, Y.H., Lee, Y.J., Choi, J., Kim, C.H., Han, D.C., and Kwon, B.M. (2019). 2'-Hydroxycinnamaldehyde inhibits proliferation and induces apoptosis via signal transducer and activator of transcription 3 inactivation and reactive oxygen species generation. *Cancer Sci*, **110**, 366–378.
- Yvan-Charvet, L., Wang, N., and Tall, A.R. (2010). Role of HDL, ABCA1, and ABCG1 transporters in cholesterol efflux and immune responses. *Arterioscler Thromb Vasc Biol*, **30**, 139–143.
- Zhao, S., Li, J., Wang, L., and Wu, X. (2016). Pomegranate peel polyphenols inhibit lipid accumulation and enhance cholesterol efflux in raw264.7 macrophages. *Food Funct*, **7**, 3201–3210.
- Zhao, T., Sun, Q., Marques, M., and Witcher, M. (2015). Anticancer Properties of *Phyllanthus emblica* (Indian Gooseberry). *Oxid Med Cell Longev*, **2015**, 950890.

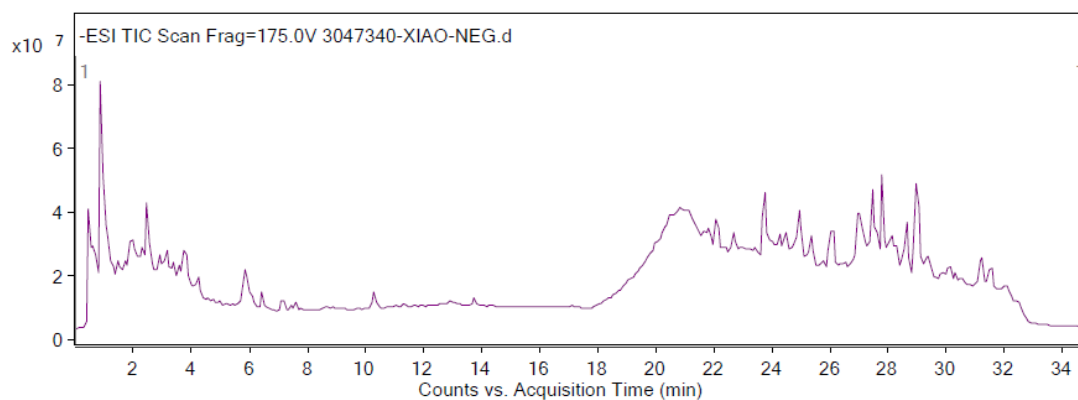
**Fruit of *Phyllanthus emblica* L. suppresses macrophage foam-cell  
genesis and vascular lipid deposition using *in vivo* and *in vitro* models  
of early atherosclerosis development**

**SUPPLEMENTARY DATA**

sFigure 1. Chromatogram of E-EA from QTOF-LC/MS run in negative mode.

sFigure 2. Chemical structure of the top 10 abundant compounds identified in E-EA by QTOF-LC/MS.

sFigure 3-12. Chromatogram and mass spectrogram of each of the top 10 abundant compounds identified.



sFigure 1. Chromatogram of E-EA from QTOF-LC/MS run in negative mode.

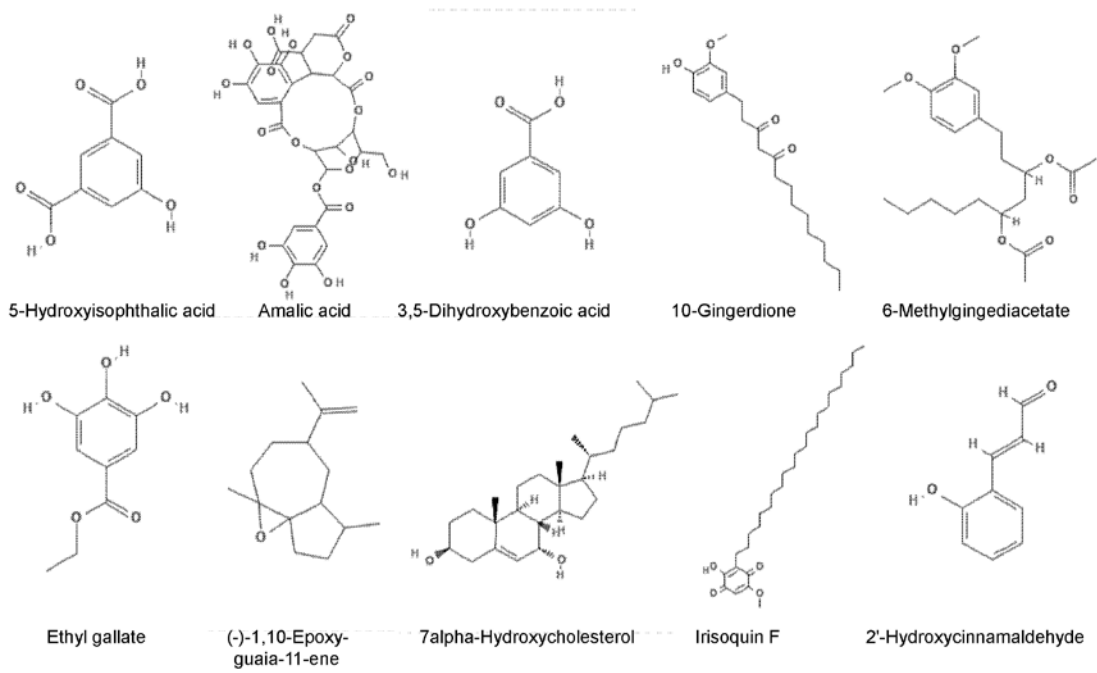
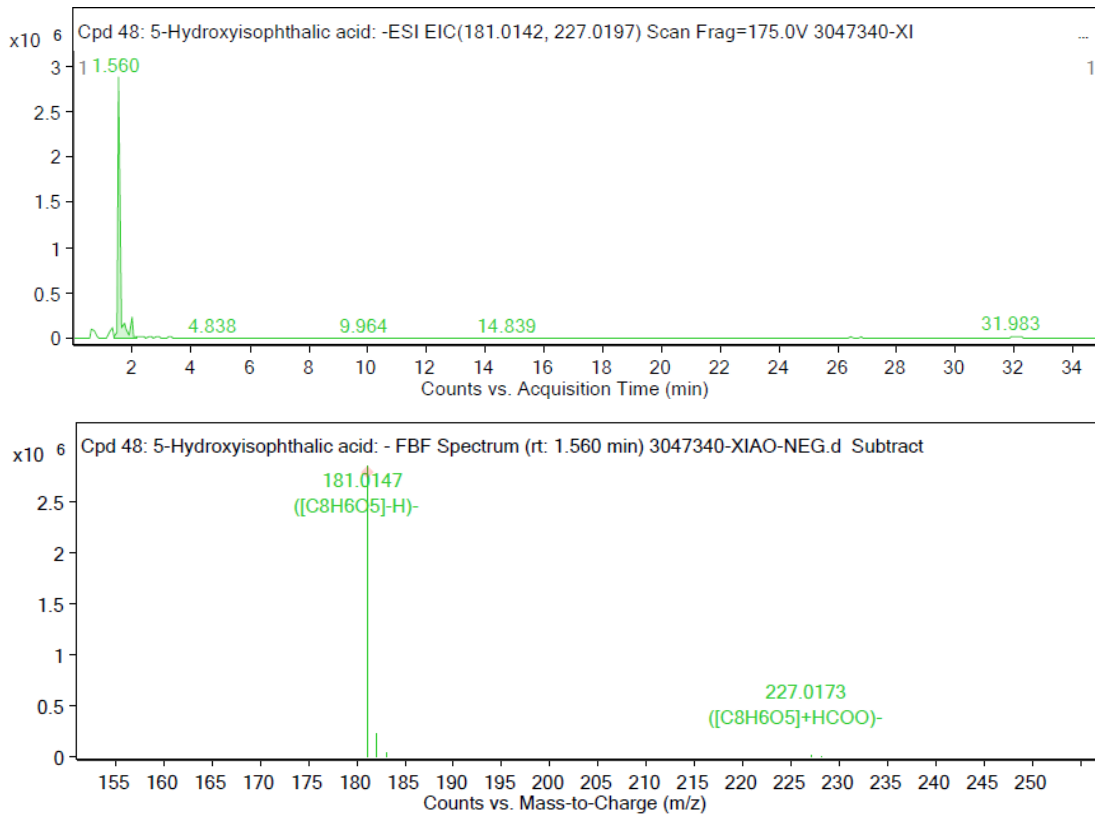


Figure 2. Chemical structure of top 10 abundant compounds identified by HPLC-MS in E-EA.



sFigure 3. Chromatogram and mass spectrogram of identified 5-Hydroxyisophthalic acid.

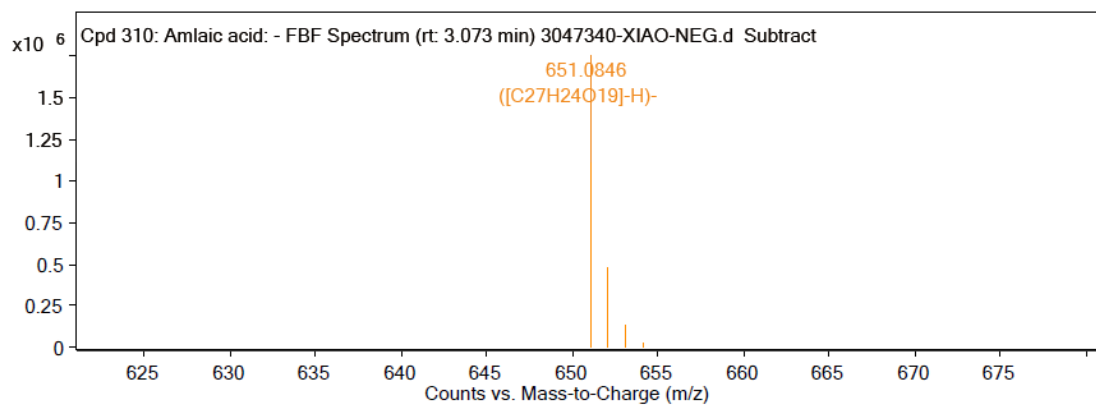
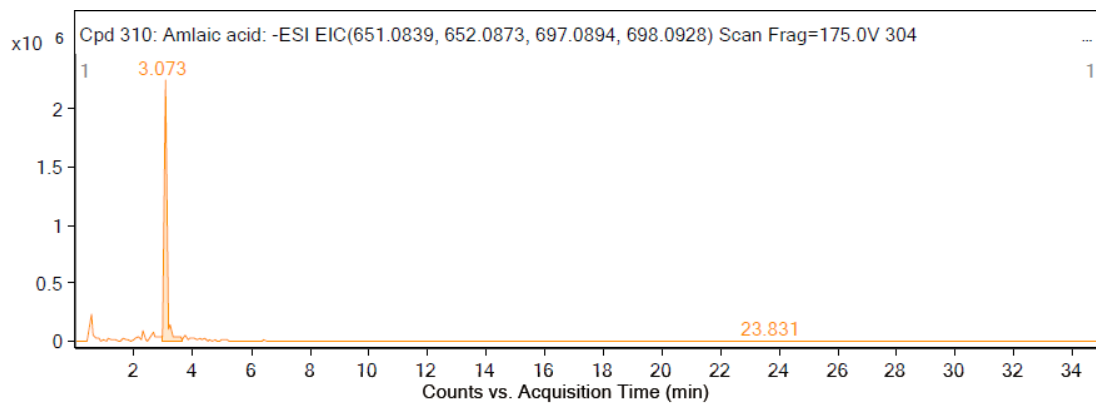
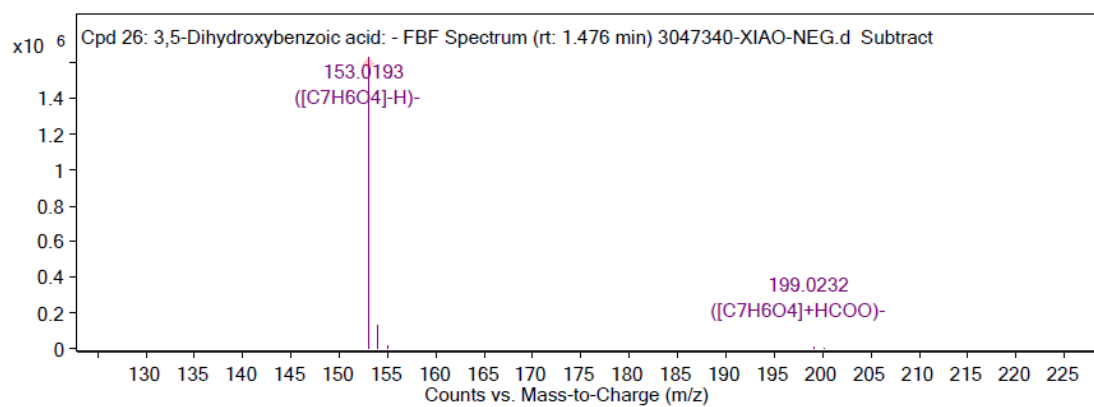
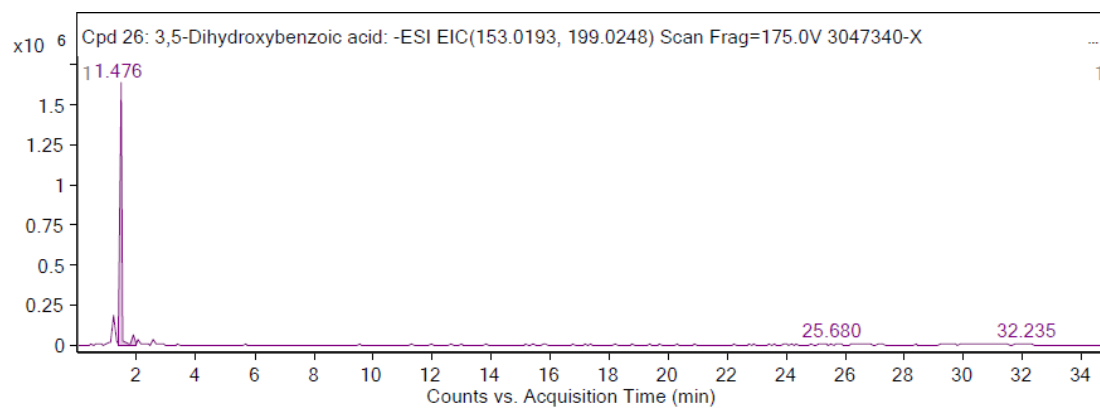


Figure 4. Chromatogram and mass spectrogram of identified amlaic acid.



sFigure 5. Chromatogram and mass spectrogram of identified 3,5-Dihydroxybenzoic acid.

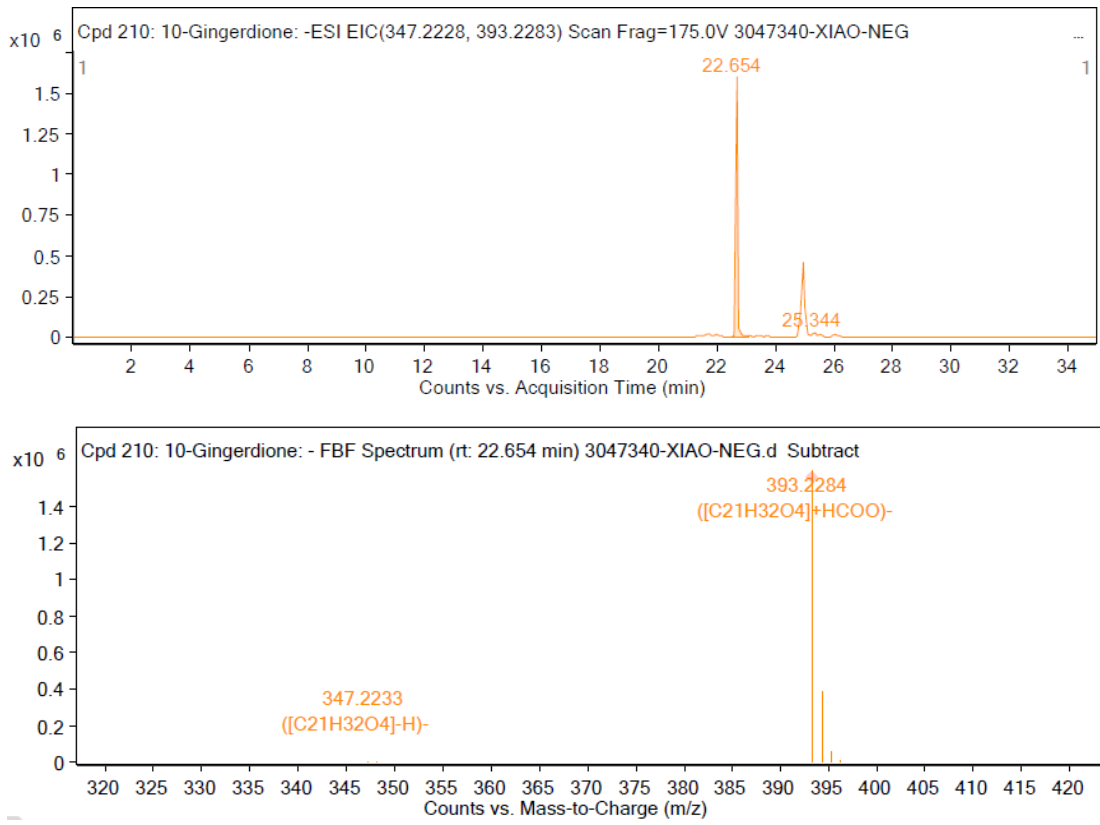


Figure 6. Chromatogram and mass spectrogram of identified 10-Gingerdione.

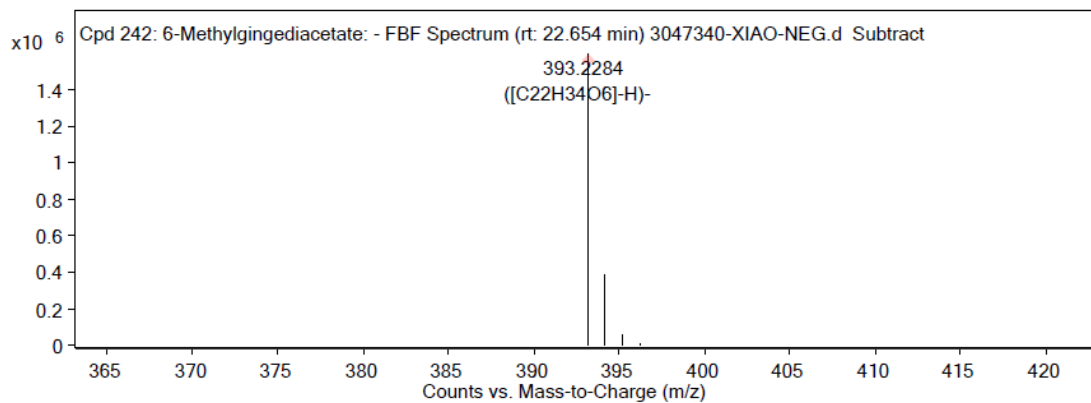
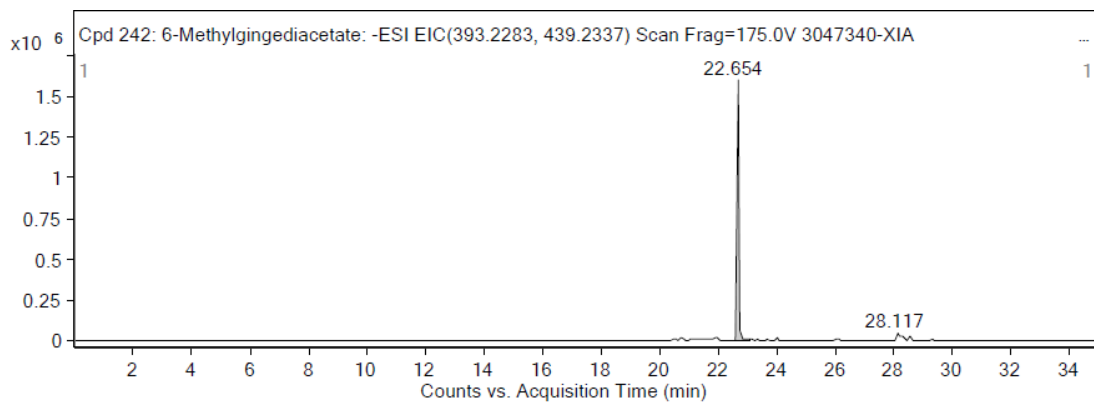
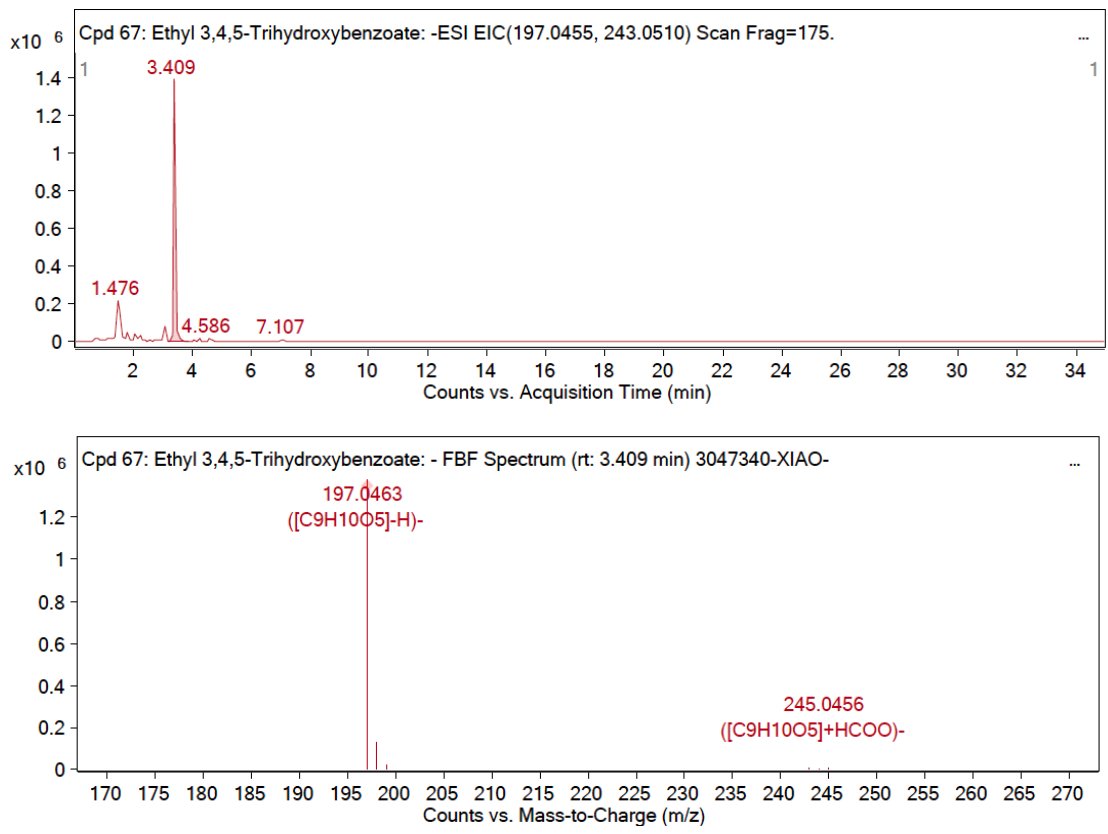


Figure 7. Chromatogram and mass spectrogram of identified 6-Methylgingediacetate.



sFigure 8. Chromatogram and mass spectrogram of identified ethyl gallate.

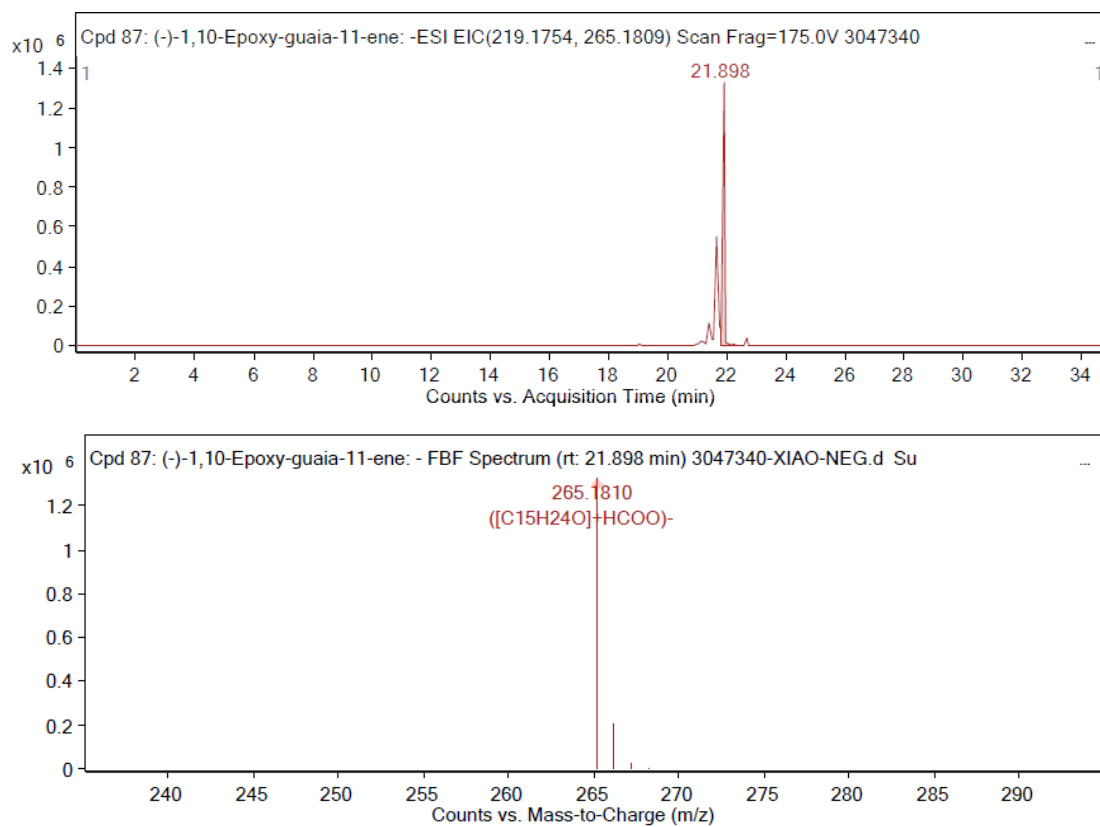


Figure 9. Chromatogram and mass spectrogram of identified (-)-1,10-Epoxy-guaia-11-ene.

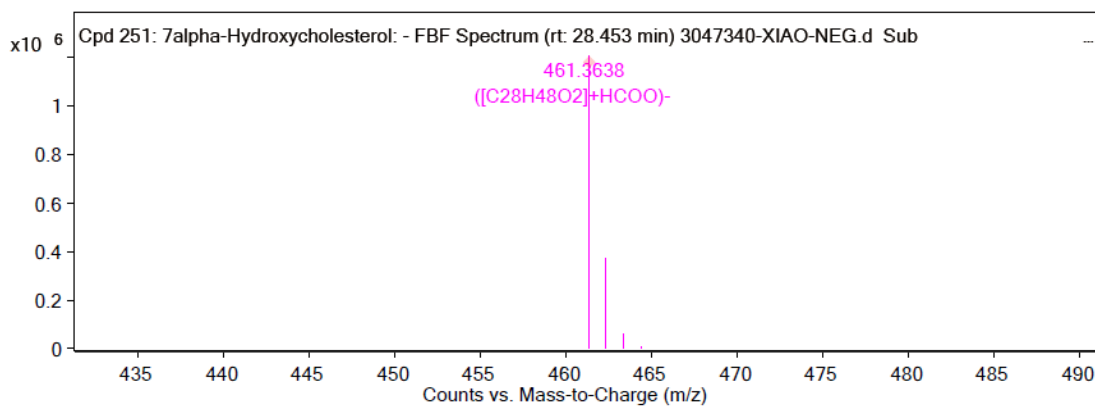
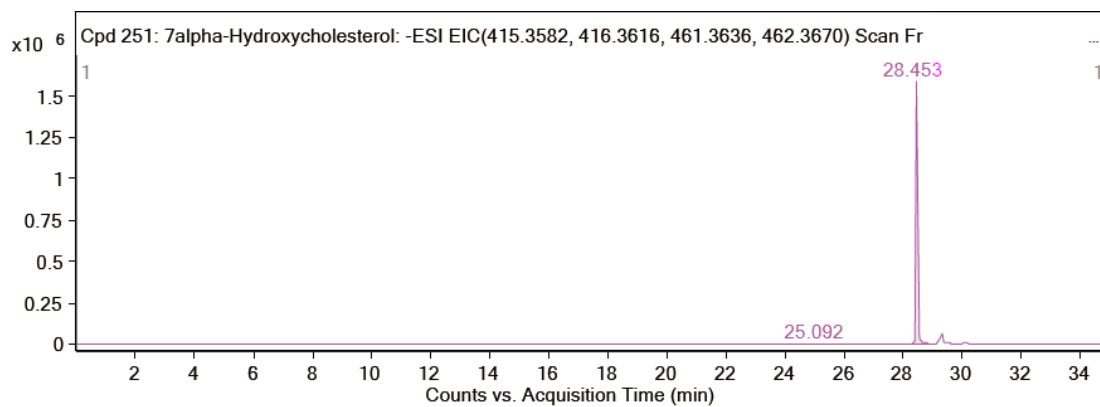
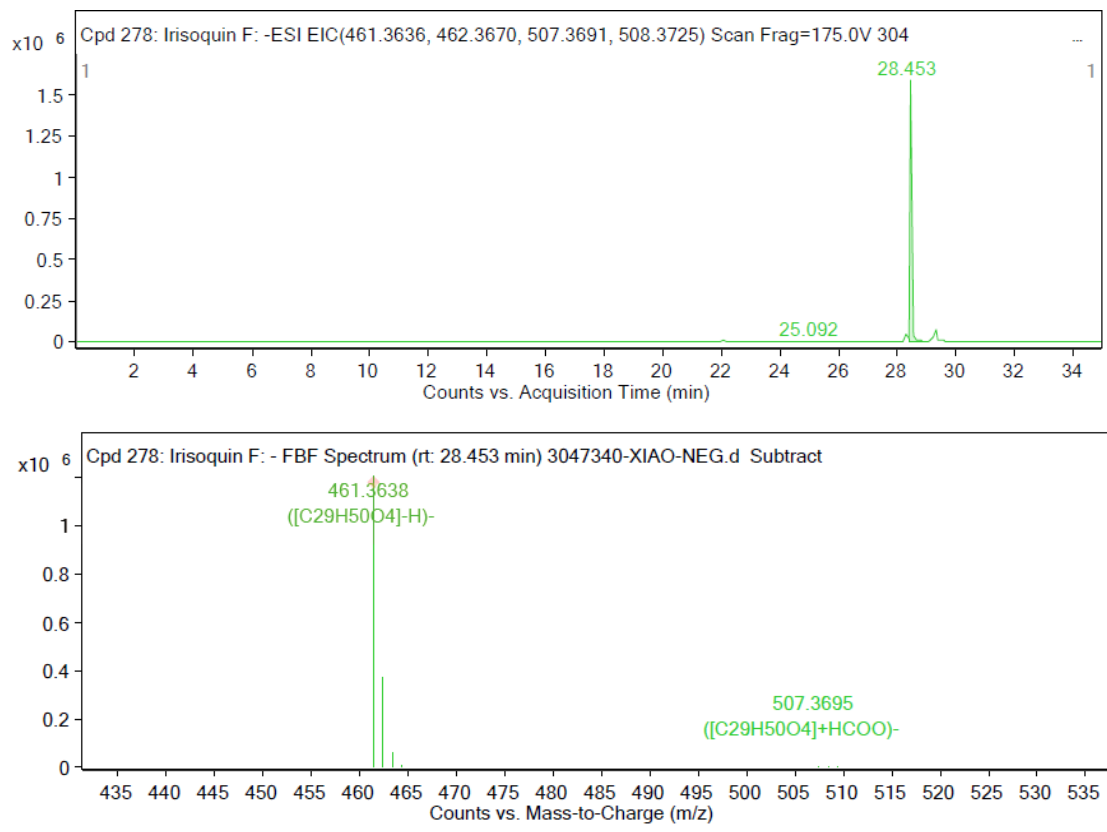


Figure 10. Chromatogram and mass spectrogram of identified 7 $\alpha$ -Hydroxycholesterol.



sFigure 11. Chromatogram and mass spectrogram of identified irisoquin F.

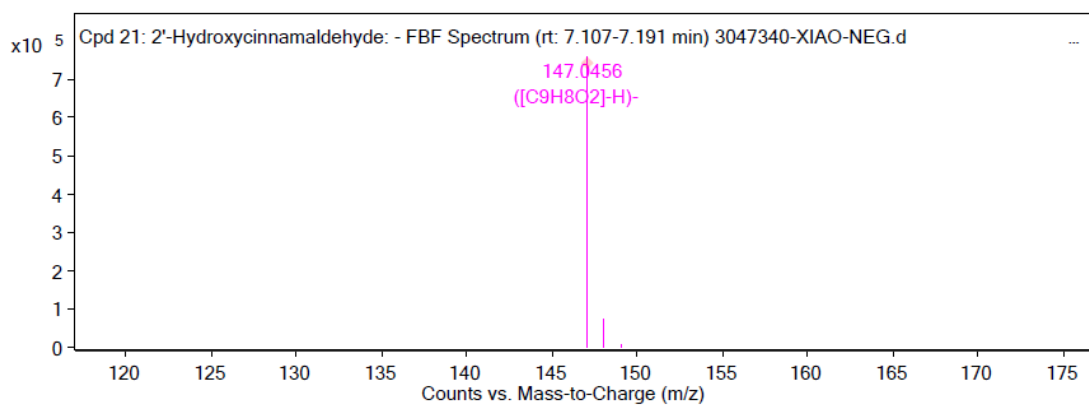
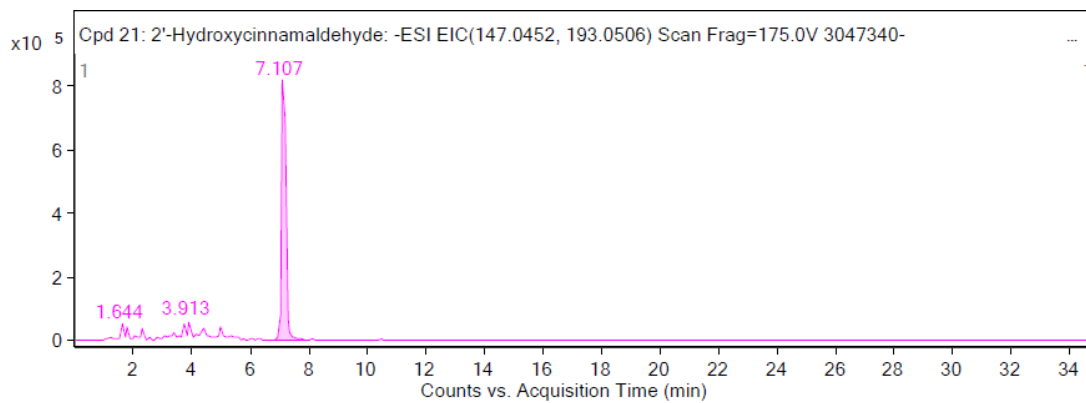


Figure 12. Chromatogram and mass spectrogram of identified 2'-Hydroxycinnamaldehyde.